Some Theoretical Studies on Physics and Astrophysics of Crustal Matter of Strongly Magnetised Compact Stars

Nandini Nag

Department of Physics, Visva-Bharati, Santiniketan

for

Pre-Ph.D. Seminar, Department of Physics 2013

Contents

- Introduction.
- A brief introduction of Thomas-Fermi & Thomas-Fermi Dirac model.
- Non-relativistic Thomas-Fermi model in presence of strong magnetic field.
- Relativistic Thomas-Fermi model in presence of strong magnetic field.
- Inner crust matter of strongly magnetized neutron stars.
- Expulsion of magnetic flux lines from super-conducting quark matter core and possible magnetic field structure at the crust.
- Conclusions.

List of publications

1. Thomas-Fermi-Dirac Model for Low Density Stellar Matter in Presence of a Strong Quantizing Magnetic Field, Int. Jour. Mod. Phys. **D11** (2002) 817.

2. The Upper Limit of Magnetic Field Strength in Dense Stellar Hadronic Matter, Astrophysics & Space Science **310**, (2007) 195.

3. The Study of Relatively Low Density Stellar Matter in Presence of Strong Quantizing Magnetic Field, Ann. of Phys., **324**, (2009) 499.

4. On a Possible Mechanism of Low Surface Magnetic Field Structure of Quark Stars, Astrophysics & Space Science, **323**, (2009) 123.

5. On the Crustal Matter of Magnetars, Euro. Phys. Jour. **A45**, (2010) 99.

Introduction

- A typical neutron star: $R \sim 20$km in diameter and mass $M \sim 1.4 M_{\odot}$.

- Neutron stars are one of the possible ends for a star. They result from massive stars of mass $> 8 M_{\odot}$. After these stars have finished burning their nuclear fuel, they undergo a supernova explosion. This explosion blows off the outer layers of a star into a beautiful supernova remnant. The central region of the star collapses under gravity. It collapses so much that protons and electrons combine to form neutrons. Hence the name **neutron star**.

- Neutron stars may appear in supernova remnants, as isolated objects, or in binary systems.

Remnant	Progenitor	Remnant mass	Size	Density	Means of support	Final state
WD	$< 8M_\odot$	$< 1.4M_\odot$	$R_\oplus$	1t/cm^3	e^-	PN
NS	$8M_\odot \leq M \leq 20M_\odot$	$< 3M_\odot$	10km	200 mt/cm^3	n	SN
BH	$> 20M_\odot$	$> 3M_\odot$	0*	∞	none	?

*Schwarzschild radius:

$$R_s = \frac{2MG}{c^2}$$

WD$\longrightarrow$ White dwarf, NS$\longrightarrow$ Neutron star, BH$\longrightarrow$ Black hole, PN$\longrightarrow$ Planetary nebula, SN$\longrightarrow$ Supernova.

Table-I

(Shapiro & Teukolsky, 1983)

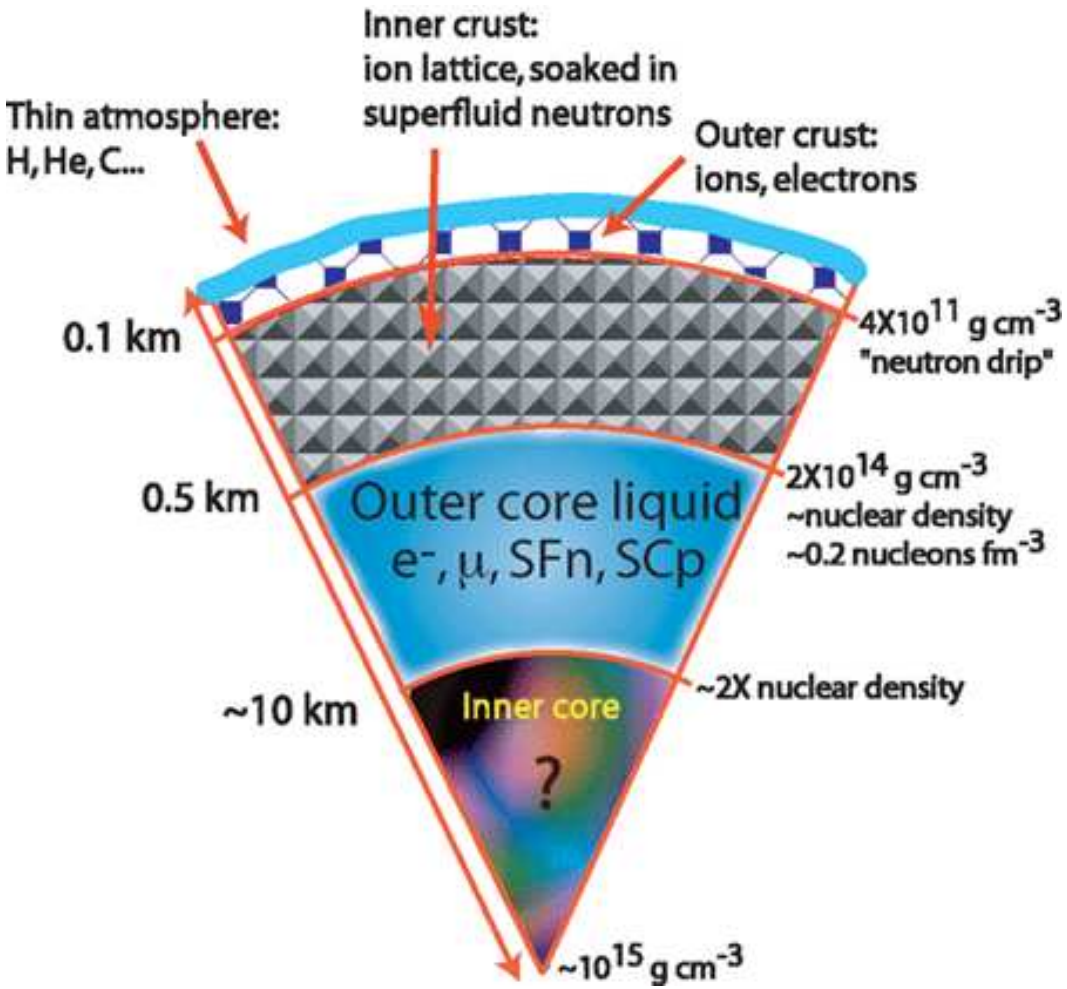

Schematic picture of neutron star's interior

A brief introduction to Thomas-Fermi & Thomas-Fermi Dirac model.

(Bertone & Ruffini, 2008 and references therein)

- Thomas-Fermi model is a semiclassical approximation. The Thomas-Fermi model assumes that the electrons of an atom constitute a fully degenerate gas of electrons confined in a spherical region by the Coulomb potential of a point-like nucleus of charge $+eN_p$. The spherical regions are called Wigner-Seitz (WS) cells.

- The condition of equilibrium (Thomas-Fermi condition) in the non-relativistic limit:

$$\frac{(P_e^F)^2}{2m_e} - eV = E_e^F \text{ constant}$$

- Assuming $eV(r) + E_e^F = e^2 Z \frac{\phi(r)}{r}$ and introduce dimensionless radial coordinate: $r = b\eta$, the constant

$$b = (3\pi)^{2/3} \frac{\hbar^2}{m_e e^2} \frac{1}{2^{7/3}} \frac{1}{Z^{1/3}}.$$

- Thomas-Fermi equation:

$$\frac{d^2\phi(\eta)}{d\eta^2} = \frac{\phi(\eta)^{3/2}}{\eta^{1/2}},$$

- Boundary conditions to solve this equation:

(I) Electric field on the nuclear surface:

$\phi' = 0$ for point nucleus and $\phi' = \frac{E_e^F R_n}{Ze^2}$ for nucleus of finite size.

(II) At the surface of WS cell, the electric field vanishes: $\Longrightarrow$

$$\phi'(\eta_s) = \frac{\phi(\eta_s)}{\eta_s}$$

The Thomas-Fermi-Dirac model

- Dirac has introduced modifications to the original Thomas-Fermi theory to include the effects of exchange interaction. This is also a semiclassical model.

- Thomas-Fermi condition:

$$\frac{(P_e^F)^2}{2m_e} - eV - \frac{\alpha}{\pi} c P_e^F = E_e^F,$$

- With $r = b\eta$, TF equation:

-

$$\frac{d^2\phi(\eta)}{d\eta^2} = \eta \left[d + \left(\frac{\phi(\eta)}{\eta} \right)^{1/2} \right]^3,$$

- Where $d = (3/(32\pi^2))^{1/3}(1/Z)^{2/3}$.

The relativistic Thomas-Fermi model

- The relativistic generalization of the equilibrium condition: $E_e^F = \sqrt{(P_e^F c)^2 + m_e^2 c^4} - m_e c^2 - eV(r) = \text{constant} > 0$

- Adopting an extended-nucleus with a radius: $R_c = r_0 A^{1/3}$, $r_0 = 1.12$fm:

- Thomas-Fermi equation:

$$\frac{1}{3x}\frac{d^2\chi(x)}{dx^2} = -\alpha\theta(x_c - x) + \frac{4\alpha}{9\pi}\left[\frac{\chi^2(x)}{x^2} + 2\frac{m_e}{m_\pi}\frac{\chi}{x}\right]^{3/2},$$

- where $x = r/\lambda_\pi$, $x_c = R_c/\lambda_\pi$, $\chi/r = e\hat{V}(r)/(c\hbar)$, $\lambda_\pi = \hbar/(m_\pi c)$ and $e\hat{V} = eV + E_e^F$.

The relativistic Thomas-Fermi-Dirac model

- With exchange corrections: $E_e^F = \sqrt{(cP_e^F)^2 + m_e^2c^4} - m_ec^2 - eV - \frac{\alpha}{\pi}cP_e^F =$ constant > 0

- The relativistic version of Thomas-Fermi-Dirac equation:

$$\frac{1}{3x}\frac{d^2\chi(x)}{dx^2} = -\frac{\alpha}{\Delta^3}\theta(x_c - x) + \frac{4\alpha}{9\pi}\{\gamma\left(\frac{m_e}{m_\pi} + \frac{\chi}{x}\right) + \left[\left(\frac{\chi}{x}\right)^2 + 2\frac{m_e}{m_\pi}\frac{\chi}{x}\right]^{1/2}$$
$$\left[\frac{(1+\gamma^2)(m_e/m_\pi + \chi/x)^2 - (m_e/m_\pi)^2}{(m_e/m_\pi + \chi/x)^2 - (m_e/m_\pi)^2}\right]^{1/2}\}^3,$$

Non-relativistic Thomas-Fermi model in presence of strong magnetic field

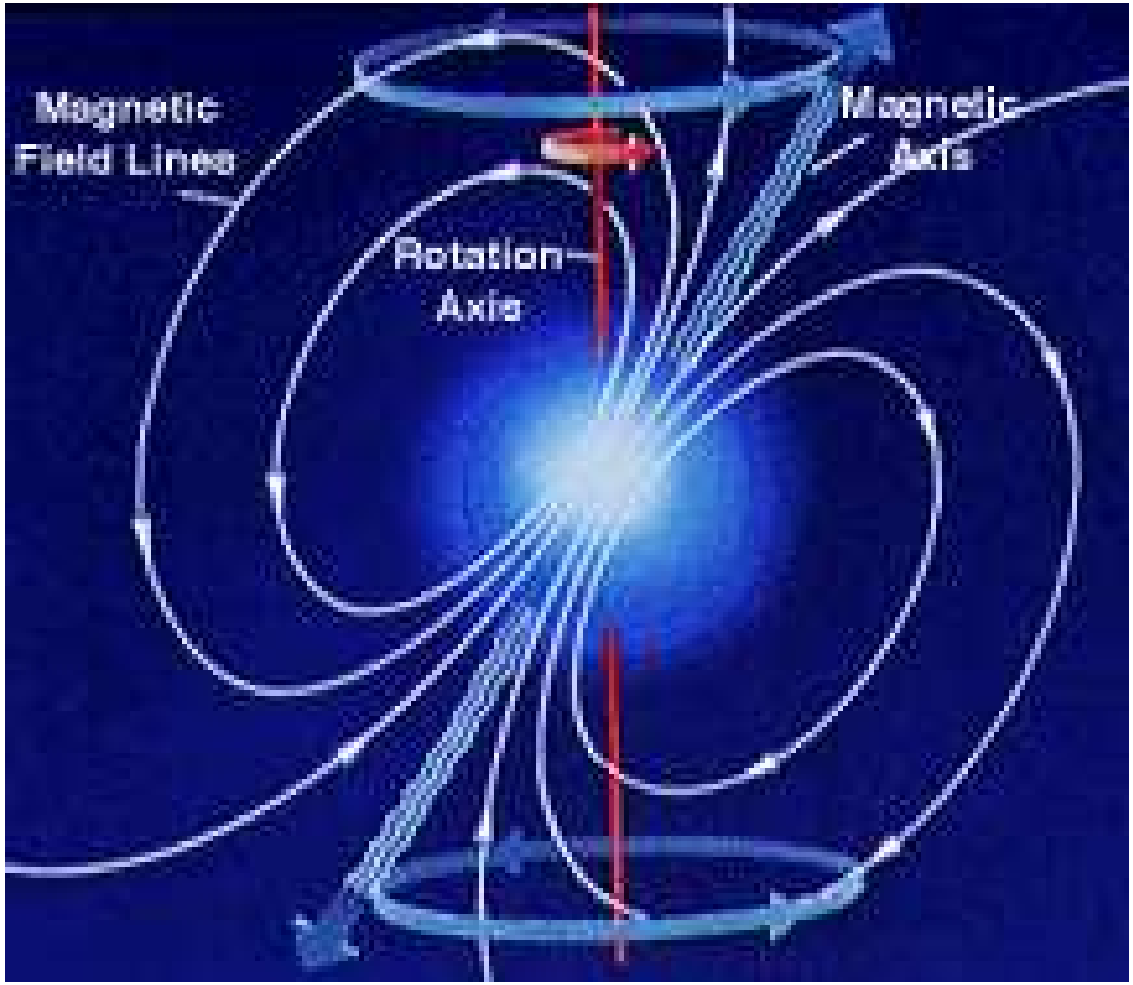

Charged Particles in Ultra-strong magnetic field

(Lieb, Solovej, Yngvason, Comm. Math. Phys., 1994)

- Motion of electrons in strong magnetic field: if Cyclotron Quantum $\geq$ Rest Mass Energy: A new effect: the Quantum Mechanical effect of strong magnetic field- called Landau Diamagnetism. For electron the critical field $\sim 4.4 \times 10^{13}$ Gauss.
  $B_c^{(e)} = \frac{m_e^2 c^3}{\hbar i |e|}$

- If $B \geq B_c^{(e)}$ phase space -spherical $\longrightarrow$ cylindrical- momentum along $\vec{B}$- continuous $(-\infty \leq p_z \leq +\infty)$, in the $\perp$-plane- momentum gets quantized- $(p_\perp = (2\nu eB)^{1/2} = (2\nu m\hbar\omega)^{1/2})$- Landau quantization, $(\nu = 0, 1, 2, ..)$-

- Energy Eigen Value: (NR)

$$E_\nu = \frac{p_z^2}{2m} + (\nu + \frac{1}{2})\hbar\omega = \frac{p_z^2}{2m} + \frac{p_\perp^2}{2m}, \quad \omega = \frac{eB}{2mc}$$

Energy Eigen Value: (R)

$$E_\nu = (p_z^2 c^2 + m^2 c^4 + 2\nu\hbar ceB)^{1/2}$$

Here $p_\perp = (2\nu\hbar ceB)^{1/2}$.

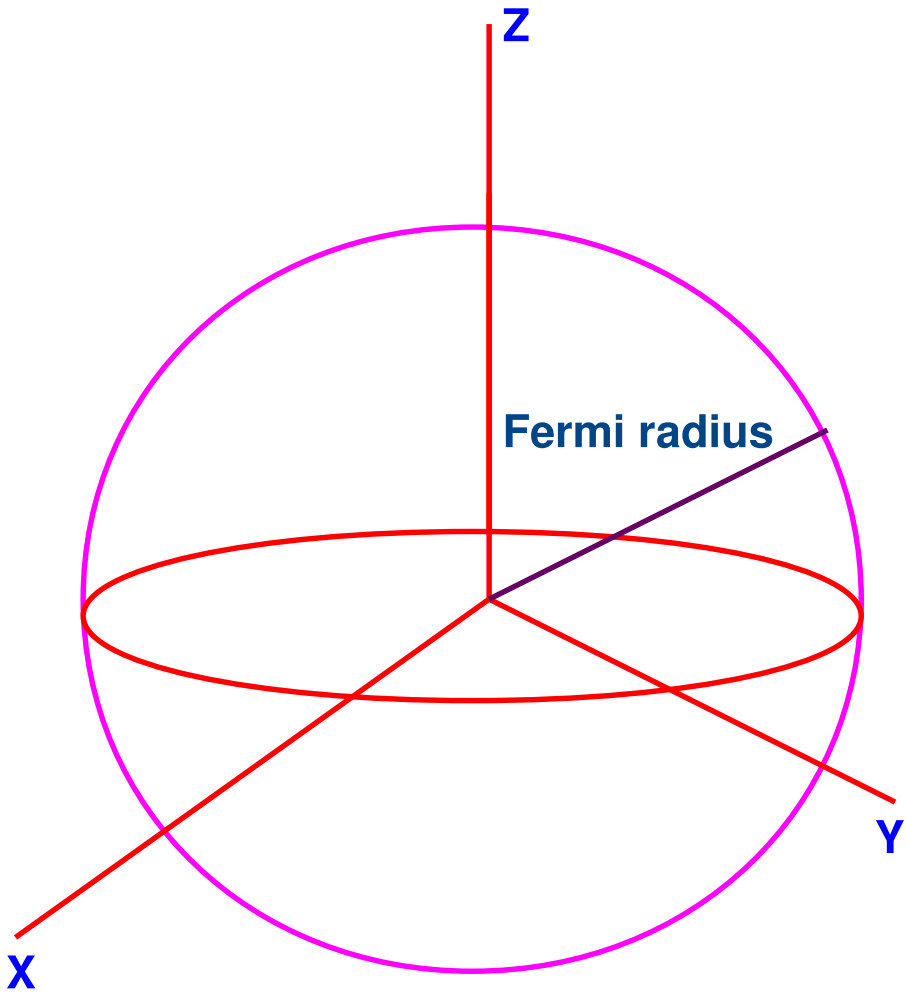

Fermi sphere: $B = 0$ or $< B_c^{(e)}$

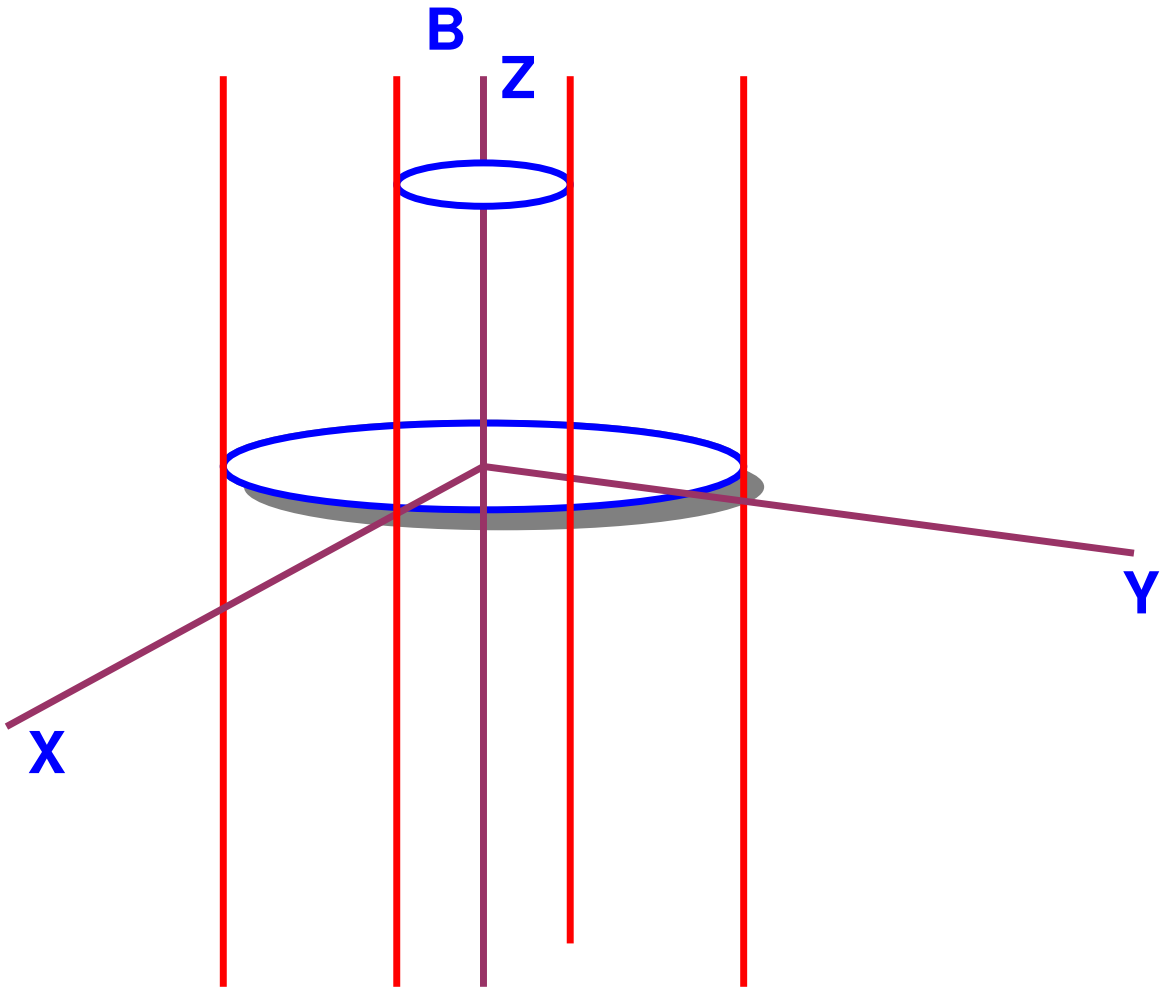

Fermi cylinder: $\geq B_c^{(e)}$

- Fermi Integral: (B is along z-axis)[Natural units: $\hbar = k_B = c = 1$]

$$I = g\frac{1}{(2\pi)^3}\int d^3p f(p) \text{ for } B = 0 \text{ or } B < B_c^{(e)} \text{ and}$$

$$I = g\frac{eB}{(2\pi)^2}\sum_{\nu=0}^{\nu_{max}}(2-\delta_{\nu 0})\int_{-\infty}^{+\infty} f(p_z,\nu)dp_z \text{ for } B \geq B_c^{(e)}$$

- For $T \neq 0$, $\nu_{max} = \infty$. For $T = 0$, limits of p_z-integral: $-p_F$ to $+p_F$.

- $(2-\delta_{\nu 0}) \longrightarrow \nu = 0$ state is singly degenerate, all others are doubly degenerate.

- For $T = 0$:

$$\nu_{max} = \frac{\mu^2 - m^2}{2eB}$$

$\mu \longrightarrow$ chemical potential.

Thomas-Fermi-Dirac model for the Outer Crust Matter of Strongly Magnetized Neutron Stars/Magnetars (non-relativistic Model)

(Nag & Chakrabarty, IJMPD)

- Outer crust matter: Dense crystal of mainly fully ionized metallic iron and degenerate electron gas

- Electron density:

$$n_e = \frac{eB}{\pi^2} p_F$$

- In Thomas-Fermi-Dirac model the electron Fermi energy:

$$\mu = \frac{p_F^2}{2m} - e\phi - u_{ex}(p_F) = \text{constant}$$

- $u_{ex} \longrightarrow$ the exchange part of electron-electron interaction: In the non magnetic case:

$$u_{ex}(p_F) = \frac{e^2}{\pi\hbar} p_F$$

- With quantising magnetic field:

$$u_{ex}(p_F) = \alpha(1 - e^{-\beta p_F})$$

- Where $\alpha(B)$ and $\beta(B)$ are given in Table-II.

- The numerically fitted functional form of Fermi momentum: $p_F = C(\mu^* + e\phi)^\gamma$

- $\mu^* = \mu + u_{ex}(p_F)$, ($C(B)$ and $\gamma(B)$ are given in Table-II).

- Thomas-Fermi Equation:

- $$\frac{d^2u}{dx^2} = x^{1-\gamma}u^{\gamma}$$

- Where

$$\mu^* + e\phi = \frac{Ze^2}{r}u(r)$$

and

$$a^{3-\gamma} = \frac{\pi\hbar^2 c}{4CBe^{2\gamma+1}Z^{\gamma-1}}$$

- The boundary condition at the cell surface:

$$\frac{du}{dx} = \frac{u}{x}$$

- Since $\gamma < 1$ for $10^{14} G \leq B \leq 10^{17}$G $\Longrightarrow$ no singularity for TF equation.

- The numerically fitted functional of $u(x)$:

$$u(x) = \frac{u_0}{1 + \exp\{\xi(x - x_0)\}}$$

- x_s, $u_0(B)$, $\xi(B)$, $x_0(B)$ $\longrightarrow$ parameters shown in Table-II.

- The mass density ρ:

$$\rho(B) = \frac{3Am_B}{4\pi a^3 x_s^3}$$

$m_B = 1.66057 \times 10^{-24}$g, $\longrightarrow$ the effective nucleon mass.

- The expression for kinetic pressure:

$$P = \frac{eB}{\pi^2}\left[\frac{p_F^3}{3m} + \alpha \exp(\beta p_F)\left(p_F + \frac{1}{\beta}\right) - \frac{\alpha}{\beta}\right]$$

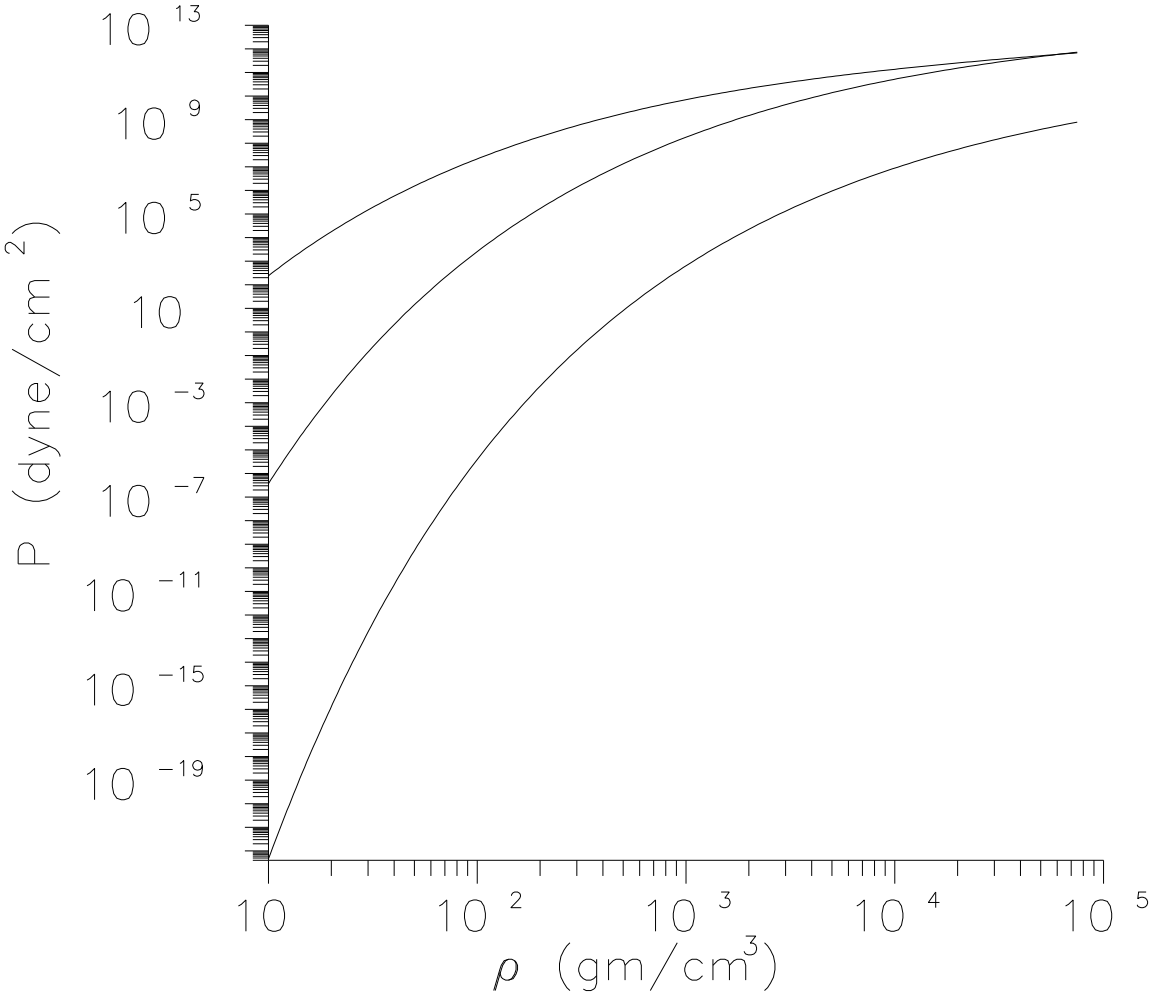

Equation of state for low density neutron star crustal matter in presence of strong magnetic fields: $B = 10^{14}$G (upper curve), $B = 10^{15}$G (middle curve) and $B = 10^{17}$G (lower curve)

Table-II

B (Gauss)	10^{14}	10^{15}	10^{17}
α (MeV)	0.568	1.796	17.909
β MeV^{-1}	3.412	1.067	0.109
γ	0.506	0.527	0.658
C	0.973	0.870	0.386
x_s	3.096	3.170	4.404
r_s (Å)	0.402	0.203	0.123
v_0	-0.938556	-0.937365	-0.936123
u_0	1.633	1.651	1.944
ξ	2.097	2.071	1.755
x_0	0.213	0.204	0.031
ρ (gm/cc)	72.79	572.29	962.14

Conclusions

- To the best of our knowledge, this is the first work on TF model in presence of strong magnetic field, when the Landau levels of the electrons are populated.

- TF equation in presence of strong magnetic field does not show singularity at the origin, which is present in the usual TF equation in absence of strong magnetic field or $B < B_c^{(e)}$ (Landau levels are not populated).

$$\text{For } B \leq B_c^{(e)} \Longrightarrow \frac{d^2u}{dx^2} = \frac{u^{3/2}}{x^{1/2}}, \quad \text{for } B > B_c^{(e)} \Longrightarrow \frac{d^2u}{dx^2} = x^{1-\gamma}u^{\gamma}$$

- Figure shows that the stability of matter at the crustal region increases with the increase in the strength of magnetic field.

Thomas-Fermi-Dirac model for the Outer Crust Matter of Strongly Magnetized Neutron Stars/Magnetars (Relativistic Model)

(Nag et al, Ann. Phys.)

- The modified form of spinor solutions of Dirac equation:

$$\psi(x) = \frac{1}{(L_y L_z)^{1/2}} \exp\{-iE_\nu t + ip_y y + ip_z z\} u^{\uparrow\downarrow}(x)$$

- where

$$u^{\uparrow}(x) = \frac{1}{[2E_\nu(E_\nu + m)]^{1/2}} \begin{pmatrix} (E_\nu + m) I_{\nu;p_y}(x) \\ 0 \\ p_z I_{\nu;p_y}(x) \\ -i(2\nu eB)^{1/2} I_{\nu-1;p_y}(x) \end{pmatrix}$$

- and

$$u^{\downarrow}(x) = \frac{1}{[2E_\nu(E_\nu + m)]^{1/2}} \begin{pmatrix} 0 \\ (E_\nu + m) I_{\nu-1;p_y}(x) \\ i(2\nu eB)^{1/2} I_{\nu;p_y}(x) \\ -p_z I_{\nu-1;p_y}(x) \end{pmatrix}$$

- where

$$I_\nu = \left(\frac{qB}{\pi}\right)^{1/4} \frac{1}{(\nu!)^{1/2}} 2^{-\nu/2} \exp\left[-\frac{1}{2}eB\left(x - \frac{p_y}{eB}\right)^2\right] H_\nu\left[(eB)^{1/2}\left(x - \frac{p_y}{eB}\right)\right]$$

- $H_\nu \longrightarrow$ Hermite polynomial of order ν.
  - Atoms are replaced by Wigner-Seitz cells
  - A and $Z \longrightarrow$ mass number and atomic number within the cell.
  - charge neutrality: $Z \longrightarrow$ number of electrons within the cell.
  - Nucleus has finite dimension: $r_n = r_0 A^{1/3}$ with $r_0 = 1.12$fm.

- Thomas-Fermi equation:

$$\nabla^2 V(r) = 4\pi e n_e(r) - 4\pi e n_p(r)\theta(r_n - r)$$

- $n_p(r) \longrightarrow$ proton density within the nucleus:

$$n_p = \frac{3Ze}{4\pi r_n^3}$$

- Thomas-Fermi Condition:

$$\varepsilon_\nu(r) - eV(r) = \text{constant} = \mu_e$$

$$\text{or} \quad (p_F^2 + m^2 + 2\nu eB)^{1/2} - eV(r) = \text{constant} = \mu_e$$

Substitute:

$$\mu_e + eV(r) = Ze^2\frac{\phi(r)}{r} \;\; \&$$

$$r = \mu x$$

- Thomas-Fermi equation $\Longrightarrow$

$$\frac{d^2\phi}{dx^2} = \sum_{\nu=0}^{\nu_{\max}} (2 - \delta_{\nu 0})(\phi^2(x) - \phi_0^2 x^2)^{1/2}$$

$$\mu = \left(\frac{\pi}{2e^3 B}\right)^{1/2} \quad \text{and} \quad \phi_0 = \frac{m_\nu \mu}{Ze^2}$$

Boundary conditions:

$$\phi(x)|_{x=x_n} = 1 \text{ and } \frac{d\phi(x)}{dx}|_{x=x_s} = \frac{\phi(x)}{x}|_{x=x_s}.$$

- Further, the right hand side of the final form of the Poisson's equation must be real. It requires, that the inequality $\phi_0 x \leq \phi(x)$ must be satisfied. Which after using ϕ_0 and m_ν [$= (m^2 + 2\nu eB)^{1/2}$], gives

$$\nu_{\max}(x) = \left[\frac{e^4 Z^2}{\pi x^2}\phi^2(x) - \frac{m^2}{2eB}\right] \geq 0$$

- This equation indicates that the upper limit of the Landau quantum number of the Wigner-Seitz electrons depends on its position within the cells.

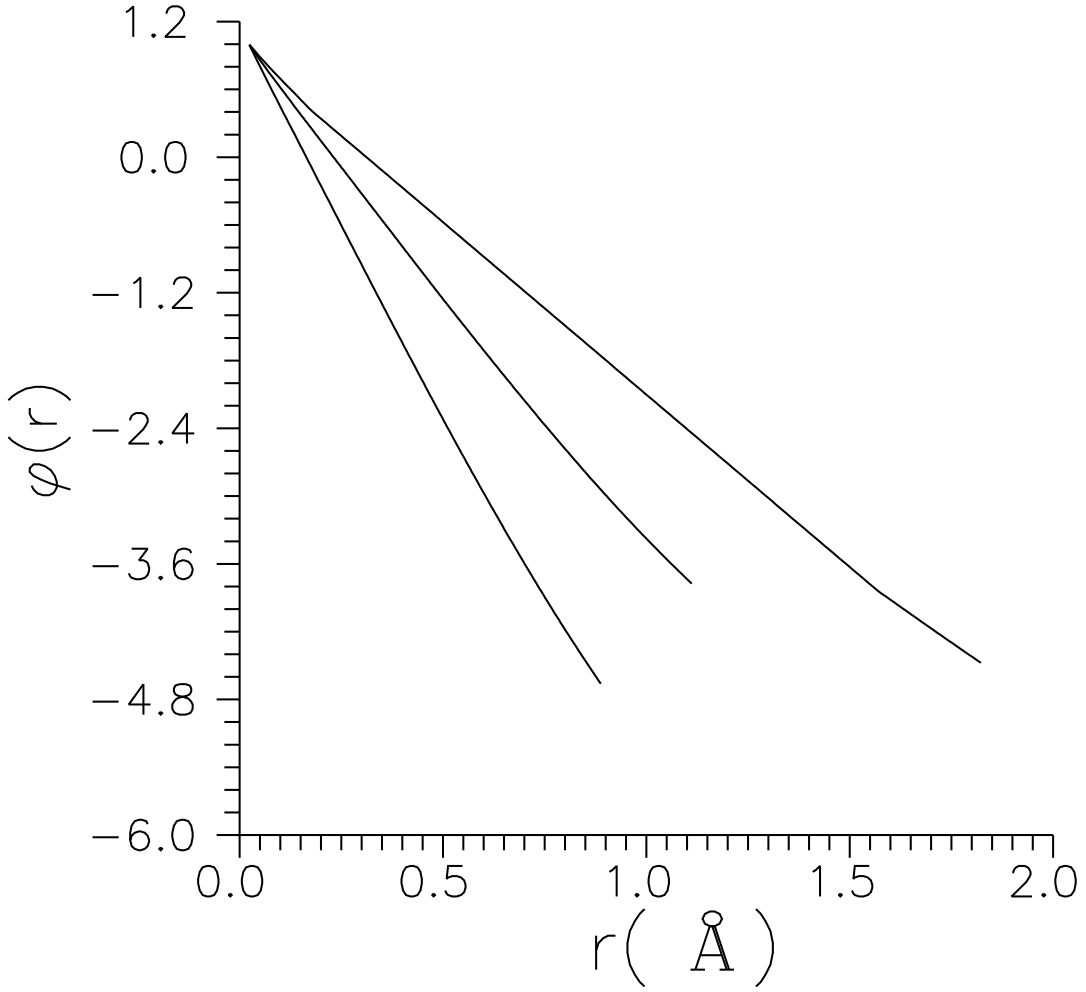

The variation of electrostatic field with radial distance from the centre, for three different initial values:$\phi'_{in} = -1.8$ (upper), $\phi'_{in} = -2.7$ (middle) and $\phi'_{in} = -5.9$ (lower). The magnetic field strength $B = 10^{14}$G

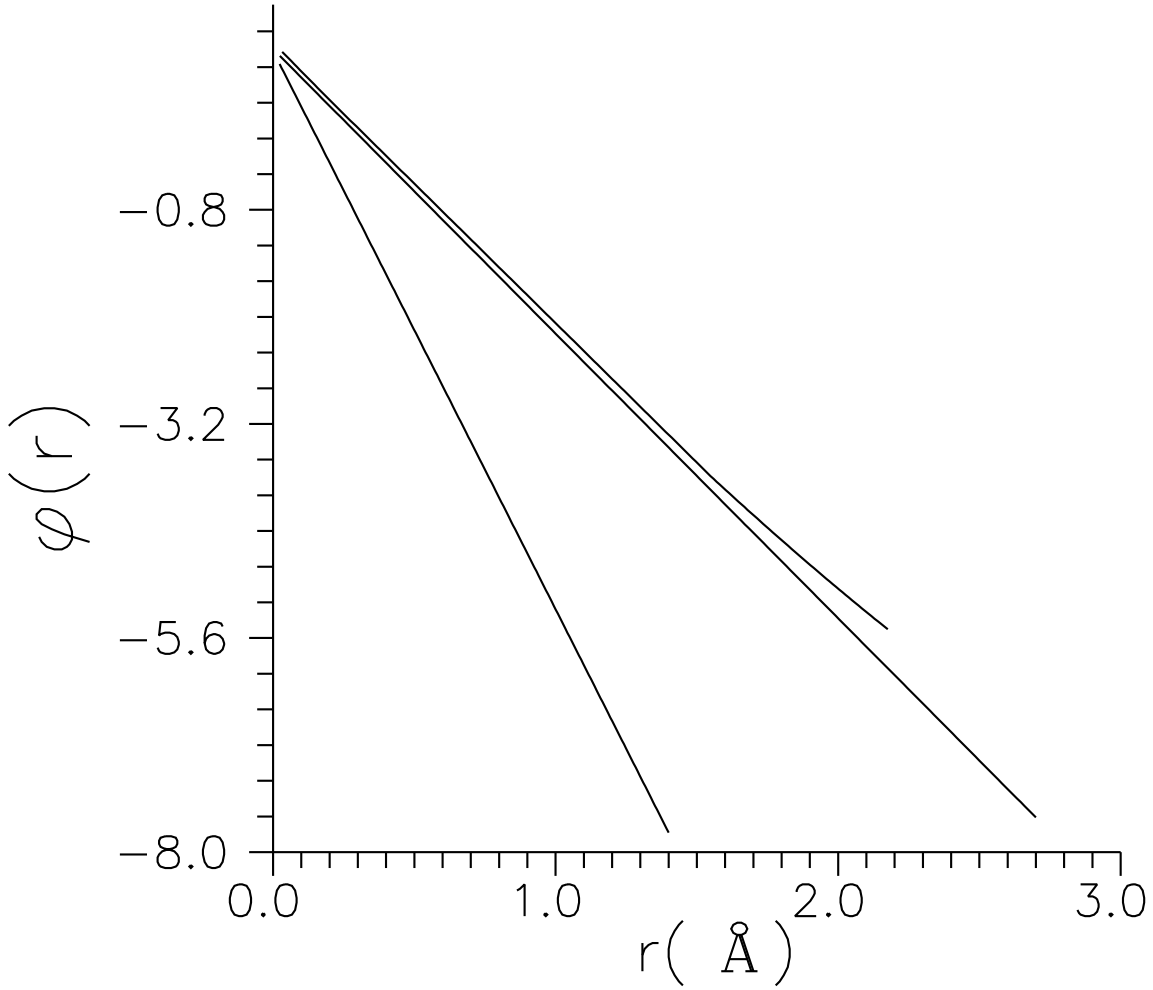

The variation of electrostatic field with radial distance from the centre, for three different magnetic field strengths: 10^{14}G (upper), 10^{15}G (middle) and 10^{17}G (lower)

- Electron Fermi Momentum:

$$p_F = [(\mu_e + eV(r))^2 - m_\nu^2]^{1/2} = \left[Z^2 e^4 \left(\frac{\phi(x_s)}{\mu x_s} \right)^2 - m_\nu^2 \right]^{1/2},$$

- Electron Number Density:

$$n_e = \frac{eB}{2\pi^2} \sum_{\nu=0}^{\nu_{\max}} (2 - \delta_{\nu 0}) p_F$$

- Kinetic Pressure:

$$P = \frac{eB}{2\pi^2} \sum_{\nu=0}^{\nu_{\max}} (2 - \delta_{\nu 0}) \left[p_F (p_F^2 + m_\nu^2)^{1/2} - m_\nu^2 \ln \left(\frac{p_F + (p_F^2 + m_\nu^2)^{1/2}}{m_\nu} \right) \right]$$

- Mass density of the crustal region of neutron stars:

$$\rho(x_s) = \epsilon(x_s) = \frac{3 A m_B}{4\pi \mu^3 x_s^3}$$

- Electron Kinetic Energy:

$$E_{KE} = \frac{eB}{\pi}\int_{r_n}^{r_s} d^3r \sum_{\nu=0}^{\nu_{\max}} (2-\delta_{\nu 0}) r^2 dr [p_F(p_F^2+m_\nu^2)^{1/2} + m_\nu^2 \ln\left(\frac{p_F+(p_F^2+m_\nu^2)^{1/2}}{m_\nu}\right) - 2mp_F]$$

- Interaction Energies:

  Electron-Nucleus Interaction Part:

$$E_{en} = -Ze^2\int_{r_n}^{r_s} d^3r \frac{n_e}{r} = -4\pi Ze^2\mu^2\int_{x_n}^{x_s} x dx n_e(x)$$

- In terms of variable x:

$$E_{en} = -\frac{Z^2 e^2}{\mu} \int_{x_n}^{x_s} d^3r \sum_{\nu=0}^{\nu_{\max}} (2 - \delta_{\nu 0}) dx (\phi(x)^2 - \phi_0^2 x^2)^{1/2}$$

- Electron-Electron Direct Interaction:

$$E_{ee}^{(d)} = \frac{1}{2} e^2 \int d^3r n_e(r) \int d^3r' n_e(r') \frac{1}{|\vec{r} - \vec{r'}|}$$

- Assuming $\vec{r}$ as the principal axis and θ is the angle between $\vec{r}$ and $\vec{r'}$. We have after evaluating the angular part:

$$\begin{aligned} E_{ee}^{(d)} &= 8e^2\pi^2 \{ \int_{r_n}^{r_s} r dr n_e(r) \int_{r_n}^{r} r'^2 dr' n_e(r') \\ &+ \int_{r_n}^{r_s} r^2 dr n_e(r) \int_{r}^{r_s} r' dr' n_e(r') \} \end{aligned}$$

- Rearranging:

$$E_{ee}^{(d)(1)} \approx \frac{Z^2e^2}{2\mu}[\frac{\alpha}{2}\left\{x_s\phi(x_s)^2 - x_n\phi(x_n)^2\right\} - \phi'(x_n)x_n\left(\phi'(x_s) - \phi'(x_n)\right) + \phi(x_n)\left(\phi'(x_s) - \phi'(x_n)\right)]$$

- where $\alpha = \nu_{\max}(\nu_{\max} + 1)$.

$$E_{ee}^{(d)(2)} \approx \frac{Z^2e^2}{2\mu}\ [\ \{(x_s\phi'(x_s) - x_n\phi'(x_n)) - (\phi(x_s) - \phi(x_n))\} - \{\ x_s(\phi'(x_s))^2 - x_n(\phi'(x_n))^2\}]$$

- Then

$$E_{ee}^{(d)} = E_{ee}^{(d)(1)} + E_{ee}^{(d)(2)}$$

- Electron-Electron Exchange Term:

- The exchange energy integral corresponding to the ith. electron in the cell:

$$E_{ee}^{(ex)} = \frac{e^2}{2} \sum_j \int d^3r d^3r' \frac{1}{|\vec{r} - \vec{r'}|} \bar{\psi}_i(\vec{r}) \bar{\psi}_j(\vec{r'}) \psi_j(\vec{r}) \psi_i(\vec{r'})$$

- $\bar{\psi}(\vec{r}) = \psi^\dagger(\vec{r})\gamma_0 \longrightarrow$ the adjoint of the spinor and $\gamma_0 \longrightarrow$ zeroth part of the Dirac gamma matrices.

  - The exact values for the exchange integrals are evaluated numerically using Monte-Carlo technique.

  - We have fitted numerically the exchange energy as a function of Fermi momentum:

$$E_{ee}(ex) = E_0^{(ex)} \exp(\alpha_{p_F})$$

- $E_0^{(ex)} = 0.043$ and 0.062 in MeV and $\alpha = 0.409$ and 0.42 in MeV^{-1} for $B = 10^{14}$G and 10^{16}G respectively.

  • It has been observed that the minimum value of p_F for which $E_{ee}^{(ex)}$ is non-zero increases with the increase in B.

  • The qualitative nature of the curves are exactly identical. However, $E_{ee}^{(ex)}$ increases with B for a given p_F.

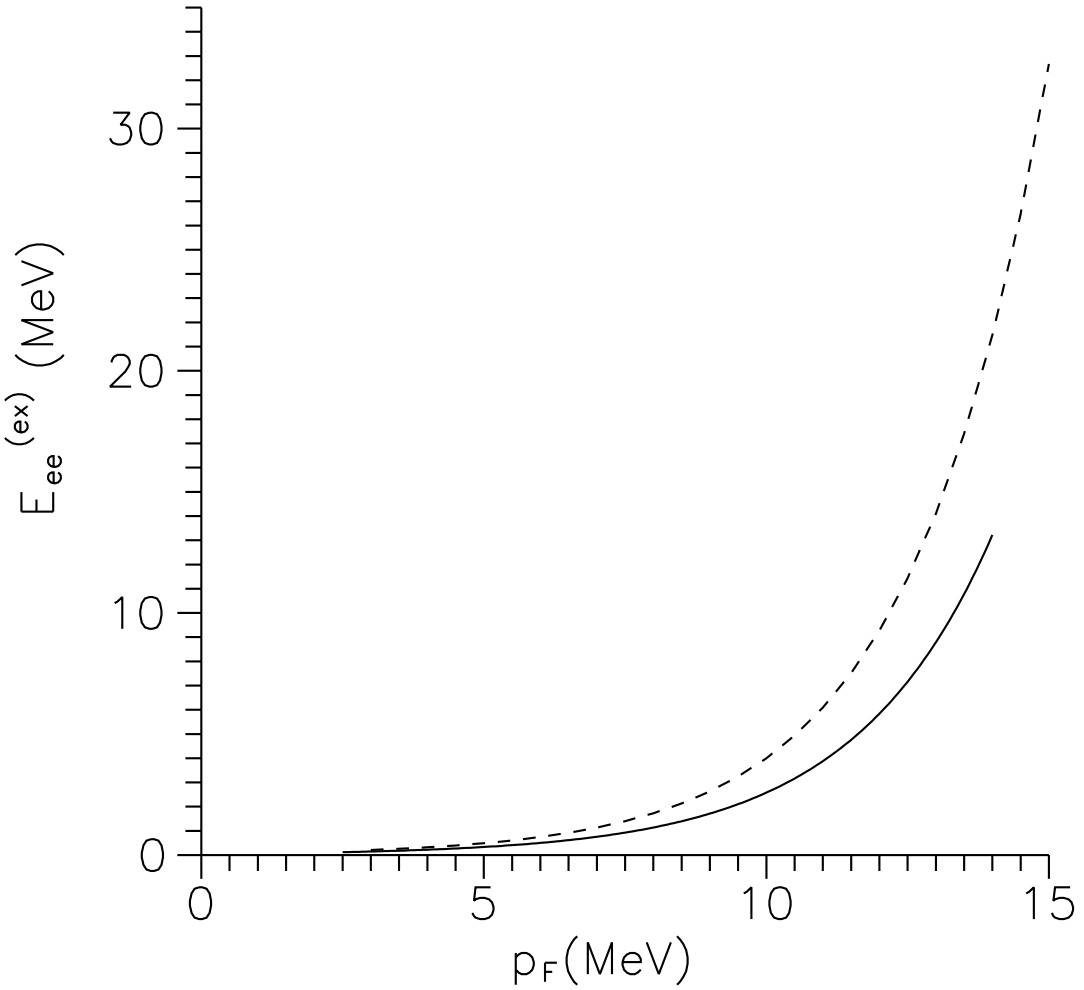

Variation of exchange energy with Fermi momentum of the electrons. The magnetic field strength $B = 10^{14}$G (solid curve) and 10^{16}G (dashed curve)

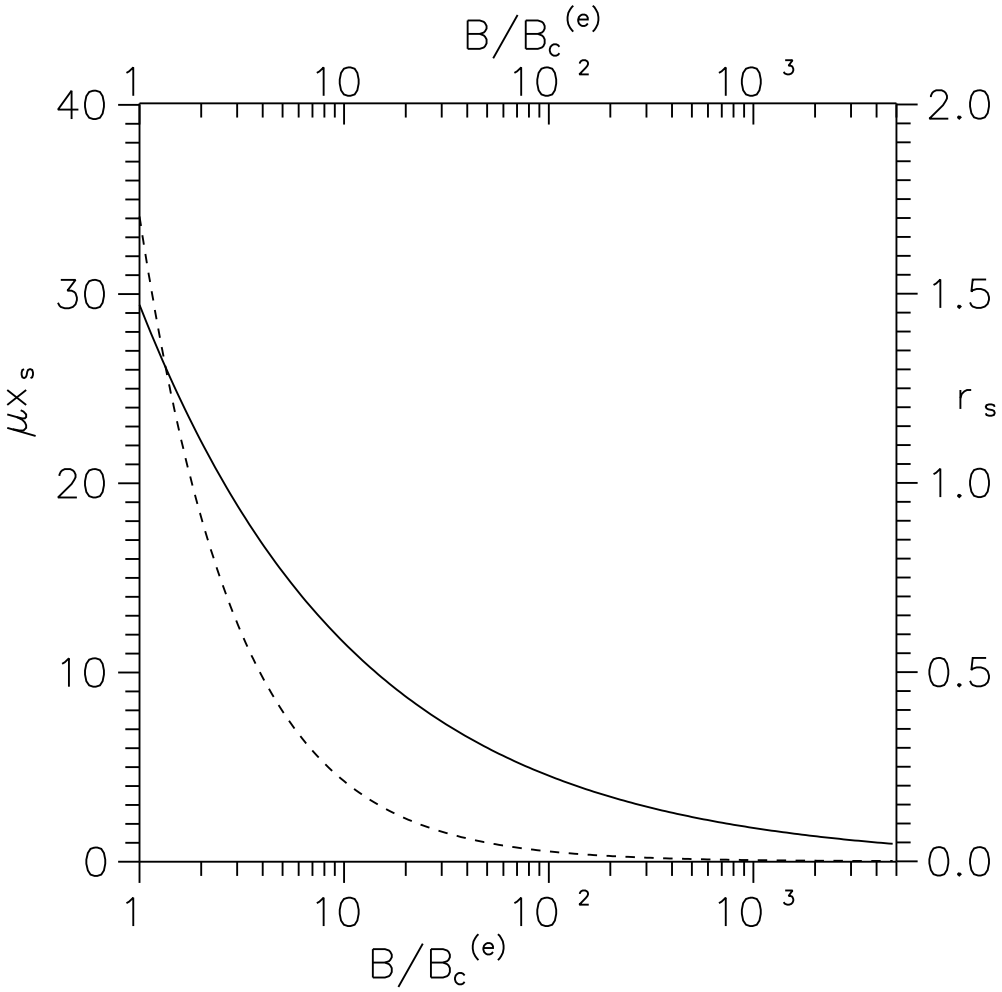

Variation of surface radius μx_s in MeV^{-1} for a typical WS cell (solid curve) and the actual radius r_s in Å unit (dashed curve) with the strength of magnetic field (expressed in terms of $B_c^{(e)}$.)

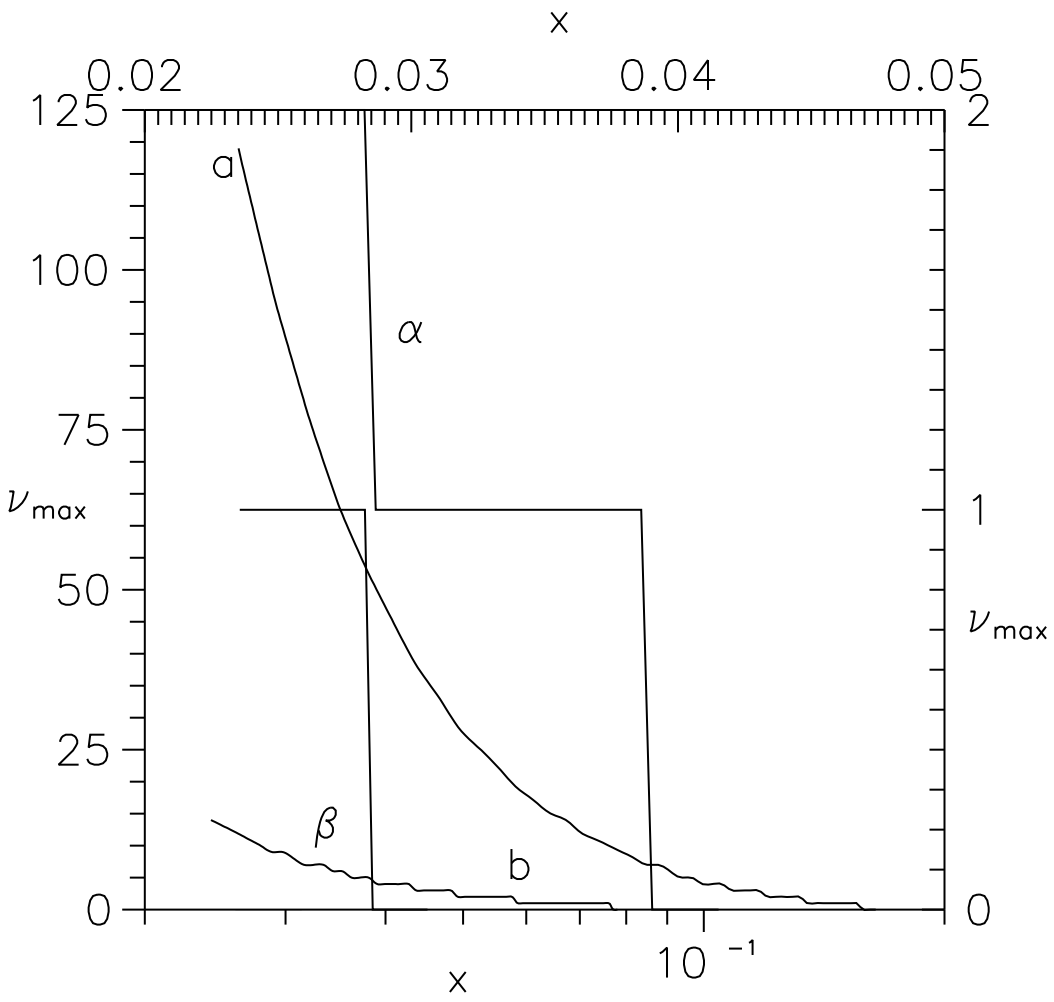

The variation of $\nu_{\max}$ with x (dimensionless). For the curves indicated by the symbols a and b, the relevant axes are at the bottom (x) and at the left side ($\nu_{\max}$), whereas for the curves represented by the symbols α and β, the axes are at the top and at the right side respectively.

Conclusions

- Using finite dimension for the nuclei, the singularity at the origin has been removed.

- In this model the radius of each WS cell decreases with the increase of magnetic field strength, the variation is $\sim B^{-1/2}$.

- To conclude our results, in the following we have given in tabular form the variation of the cell averaged values of Fermi momentum, Pressure, and various kinds of energy (except the exchange energy part) for electron gas within a typical Wigner-Seitz cell, with the strength of magnetic field.

Table-III

B/B_c	$p_F(x_s)$(MeV)	$P(x_s)$(MeV^4)	$E_{KE}(x_s)$(MeV)	$E_{en}(x_s)$(MeV)	$E_{ee}^{(d)}(x_s)$(MeV)
10^5	2.57	8.64×10^4	15.95	46.71	8.12
5×10^4	2.58	7153.02	18.13	27.15	12.15
10^4	2.66	4323.14	19.58	4.88	19.80
5×10^3	2.76	681.79	24.53	-0.37	23.82
10^3	3.56	319.78	27.30	-7.89	36.18
5×10^2	4.82	62.99	37.67	-9.69	44.55
10^2	6.95	38.06	44.81	-12.09	78.04
50	9.13	31.49	195.02	-13.13	93.95
10	13.61	10.06	781.47	-13.85	104.24
1	19.94	6.28	1.13×10^5	-35.94	130.67

- From the above tabular form of data one can see that the electron Fermi momentum and the corresponding kinetic energy decreases with the strength of magnetic field.

- Since the exchange energy is negative in nature and its magnitude increases with the magnetic field strength, we conclude that the system becomes more and more stable (total energy decreases) with the increase in magnetic field strength.

- For same B, $\nu_{\mathsf{max}}(x)$ starts with quite large values near the nuclear surface, e.g., $= 124$ and $= 15$ as shown in curves a and b respectively. Whereas, for curve α it starts with $\nu_{\mathsf{max}} = 2$ and for β, the starting value is $\nu_{\mathsf{max}} = 1$.

Inner-Crust Region

(Nag & Chakrabarty, EPJA)

- Density: $\rho \geq 10^{11}$gm cm^{-3} $\longrightarrow$ neutron drip ($\sim 4.3 \times 10^{11}$gm cm^{-3}).
- Matter: Nuclei (mainly fully ionized iron and some neutron rich heavy nuclei), free neutron gas (above neutron drip) and electron gas (for overall charge neutrality).
- Pressure: Neutron (beyond neutron drip density) and electron gas.
- Energy: Rest mass of the nuclei (normal and neutron rich)
- Equation of States:

(i) Harrison-Wheeler mass formula (HW) ($10^7 \leq \rho \leq 4 \times 10^{11}$gm cm^{-3}),

(ii) Baym-Pethick-Sutherland (BPS) mass formula ($10^7 \leq \rho \leq 3.4 \times 10^{11}$ gm cm^{-3}) (just onset of neutron drip) and

(iii) Baym-Bethe-Pethick (BBP) mass formula (neutron drip to nuclear density $\sim 10^{14}$ gm cm^{-3}).

- S.L. Shapiro and S.A. Teukolsky, Black Holes, White Dwarfs and Neutron Stars, John Wiley and Sons, New York, (1983).

- Y.S. Leung, Physics of Dense Matter, World Scientific, Singapore, (1984).

EOS for Inner Crust Matter with HW Mass Formula:

•Constituents: nuclei (normal and also neutron rich), electron gas and neutron gas (above neutron drip).

• In HW EOS, nuclei are incompressible.

•We start with the energy density of the system: $\epsilon = n_N M(A,Z) + \epsilon'_e(n_e) + \epsilon_n(n_n)$, $M(A,Z) \longrightarrow$ energy of a nucleus $\Longleftarrow$ Nuclear Mass Formula, $n_N \longrightarrow$ nuclei/vol.

• The semi-empirical nuclear mass may be written in the form:

$$M(A,Z) = [(A-Z)m_n + Z(m_p + m_e) - A\overline{E}_B]$$

• where $\overline{E}_B \longrightarrow$ mean binding energy per baryon.

• Considering all kinds of contributions:

$$M(A,Z) = m_u \left[b_1 A + b_2 A^{2/3} - b_3 Z + b_4 A \left(\frac{1}{2} - \frac{Z}{A}\right)^2 + \frac{b_5 Z^2}{A^{1/3}} \right]$$

•where $b_1 = 0.991749, b_2 = 0.01911, b_3 = 0.000840, b_4 = 0.10175, b_5 = 0.000763$ and $m_u = 1.66057 \times 10^{-24}$gm (atomic mass unit)- average baryon mass.

•Terms are: Bulk part, Surface part, Coulomb part, Iso-spin or Symmetry part, Pairing part respectively.

↓

Conventional nuclear mass formula terms

- Energy density can be re-expressed as:

$$\epsilon = n(1 - Y_n)\frac{M(A,Z)}{A} + \epsilon'_e(n_e) + \epsilon_n(n_n)$$

- Where: $n_e = n(1 - Y_n)Z/A$ and $n_n = nY_n$.

- For electron the kinetic energy density:

$$\epsilon'_e = \epsilon_e - n_e m_e$$

- Assuming A and Z as continuous variables, we have:

$$(I)\ \ \frac{\partial \epsilon}{\partial Z} = \frac{\partial}{\partial Z}\left[n_N M(A,Z) + \epsilon'_e + \epsilon_n\right] = 0$$

$$(II)\ \ \frac{\partial M}{\partial Z} = -(\mu_e - m_e)$$

- Continuous limit of $M(Z-1,A)$ with $M(Z,A)$:

- $$(III)\ \ \mu_n = \frac{\partial \epsilon_n}{\partial n_e} \ \text{and} \ \ \mu_e - m_e = \frac{\partial \epsilon'_e}{\partial n_e}$$

- $$(IV)\ \ Z\frac{\partial M}{\partial Z} + A\frac{\partial M}{\partial A} - M = 0$$

- $$(V)\ \ Z = \left(\frac{b_2}{2b_5}\right)^{1/2} A^{1/2} = 3.54 A^{1/2}$$

- Hence Z increases with A ($Z \sim A^{1/2}$), but Z/A decreases with A

- (VI)

$$b_1 = \frac{2b_2 A^{-1/3}}{3} + b_4\left(\frac{1}{4} - \frac{Z^2}{A^2}\right) - \frac{b_5}{Z^2}3A^{4/3}$$
$$= (1 + x_n^2)^{1/2}$$

- Mass density or the energy density:

$$\rho = \epsilon = n_e \frac{M(A,Z)}{Z} + \epsilon_e' + \epsilon_n$$

- Kinetic pressure: $P = P_e + P_n$ and the baryon density:

$$n = n_e \frac{A}{Z} + n_n$$

- Hence the equation of state $P \equiv P(\rho)$.

- We have noticed that at Neutron drip: $\rho \sim 3.18 \times 10^{11}$gm cm^{-3} at $(A, Z) = (122, 39.1) \longrightarrow$ Yttrium and in this density $\mu_e \sim 23.6$MeV.

- At $\rho \sim 4.54 \times 10^{12}$gm cm^{-3}, $(A, Z) = (187, 48.7)$.

- At this density $P_n/P \sim 0.6$.

- Above this density $\longrightarrow$ free $n - p - e$ mixture in β-equilibrium.

- That is

$$\begin{aligned} n_p &= n_e \\ \mu_n &= \mu_p + \mu_e \\ n &= n_p + n_n \end{aligned}$$

EOS for Inner Crust Matter with BPS Mass Formula:

- Constituents for inner Crust matter: nuclei (normal and also neutron rich), electrons in Wigner-Seitz cells, free electron gas (at high density) and neutron gas (above neutron drip):

- Energy Density of the System: $\epsilon = n_N M(A,Z) + \epsilon'_e(n_e) + \epsilon_n(n_n) + \epsilon_L$

- $\epsilon_L \longrightarrow$ Lattice energy.

- Nuclei are at regular lattice points. Around each nuclei a charge neutral cell, known as Wigner-Seitz (WS) cell is considered.

- Lattice energy:

$$\epsilon_L = n_e \frac{E_c}{Z} = n_e \frac{E_{ei} + E_{ee}}{Z} = -\frac{9}{10}\left(\frac{4\pi}{3}\right)^{1/3} Z^{2/3} e^2 n_e^{4/3} = a n_e^{4/3} \approx -1.45079 n_e^{4/3}$$

for Fe-nucleus.

- For BCC type lattice: $\epsilon_L \approx -1.44423$. The arrangement is almost BCC type, of course the density is $\sim 280\times$ normal iron density .

- Lattice contribution of pressure:

$$P_L = -\frac{d(E_c/Z)}{d(1/n_e)} = n_e^2 \frac{d}{dn_e}\left(\frac{E_c}{Z}\right) = \frac{1}{3}\epsilon_L$$

- Modified form of the Basic Equations:

$$\frac{\partial M}{\partial Z} = -(\mu_e - m_e) - 2aZ^{2/3}n_e^{1/3}, \quad \frac{\partial M}{\partial A} = \mu_n - \frac{4}{3}aZ^{5/3}n_e^{1/3}$$

and

$$Z\frac{\partial M}{\partial Z} + A\frac{\partial M}{\partial A} - M = -\frac{2}{3}aZ^{5/3}n_e^{1/3}$$

- Results: Both A and Z increase with n.

- Extra effect in the mass formula (which is quite important): the local increase in binding energy for nuclei near closed shell- known as shell effect has been taken into account.

EOS for Inner Crust Matter with BBP Mass Formula:

- Constituents for inner Crust: nuclei (normal and also neutron rich), electrons in Wigner-Seitz cells, free electron gas (at high density) and neutron gas (above neutron drip)

- Basic Assumptions:
  - Nuclei are compressible liquid drops.
  - Pressure equilibrium: Internal pressure = external pressure.
  - Chemical equilibrium inside and out side matter.
  - Effect of external matter on surface energy; surface energy vanishes when the external density of neutron matter just reaches the internal nuclear density $\longrightarrow$ the nuclei just dissolve to uniform neutron matter (with a small fraction of protons and electrons).

- Total energy density: $\epsilon = \epsilon(A, Z, n_N, n_n, V_N) = n_N(W_N + W_L) + \epsilon_n(n_n)(1 - V_N n_N) + \epsilon_e(n_e)$

- where
  - n_N: nuclei/volume.
  - n_n: free neutrons/volume.
  - V_N: volume of a nucleus (decreases as the outside pressure by n or e increases).
  - $V_N n_N$: fraction of unit volume occupied by the nuclei.
  - W_N: energy of a nucleus, including the rest mass.
  - W_L: lattice energy.
  - ϵ_n: energy of free neutron/volume.
  - ϵ_e: energy of electrons/volume.

- Chemical potentials:
  - μ_e- electrons.
  - $\mu_n^{(N)}$- neutrons inside the nuclei
  - $\mu_n^{(G)}$- neutrons in the neutron matter.
  - $\mu_p^{(N)}$- protons inside the nuclei.

- Chemical equilibrium: $\mu_p^{(N)} = \mu_e + \mu_n^{(N)}$

- $\mu_n^{(N)} = \mu_n^{(G)} \Longrightarrow$ It must cost no energy to transfer a neutron from the gas to the nucleus and vice-versa.

- Pressure equilibrium:

  $P_n^{(N)} = n_n \mu_n^{(G)} - \epsilon_n$, i.e., $P_n^{(N)} = P_n^{(G)}$

- Form of W_N:

  $$W_N = A[(1-x)m_n + xm_p + W(k,x)] + W_c + W_s$$

  - $x = Z/A$- determines $n-p$ asymmetry of the system.
  - $W(k,x)$- bulk energy of the nuclear matter / nucleon, obtained using field theoretic technique.
  - k- Fermi momentum.
  - W_c- Coulomb energy.
  - W_s - surface energy per nucleon.

- Form of W_s:

$$W_s = \frac{\sigma(W_0 - W_i)^{1/2}}{w_0^{1/2}} \frac{(n_i - n_0)^{3/2}}{n_s^{3/2}} \frac{k_0^2}{k^2} A^{2/3}$$

- where $\sigma \sim 20$MeV, $w_0 = 16.5$MeV, $k_0 = 1.43\text{fm}^{-3}$, $W_0 = W(n_0)$- bulk energy outside the nucleus and $W_i = W(n_i)$, bulk energy inside the nucleus.

- Form of W_c:

$$W_c = \frac{3}{5}\frac{Z^2e^2}{r_N}$$

  - -the energy of a uniformly charged sphere of radius r_N.

- Form of W_L:

$$W_{c+L} = \frac{3}{5}\frac{Z^2e^2}{r_N}\left(1-\frac{r_N}{r_c}\right)^2\left(1-\frac{r_N}{2r_c}\right)$$

- where r_c is given by $4\pi r_c^3 n_N/3 = 1$. In $W_c + W_L$, the Coulomb energy for electron gas is included. ϵ_e is known.

- In BBP model: for $\rho \sim 1.5 \times 10^{12}$gm cm^{-3}, $P_n/P \sim 0.20 \longrightarrow 20\%$, whereas, for $\rho \sim 1.5 \times 10^{13}$gm cm^{-3}, $P_n/P \sim 0.80 \longrightarrow 80\%$

How to get EOS?:

- Choose a value of $A \geq 56$.
- Get Z from A.
- Test whether neutron drip has been reached ($n_n > 0$)
- If $n_n > 0$, obtain ϵ_n and P_n- neutron matter energy density and pressure respectively.
- Then obtain x_e, the fractional abundance of electrons.
- Finally, obtain n_e, the electron density, ϵ'_e, the electron kinetic energy density and P_e, the electron pressure.

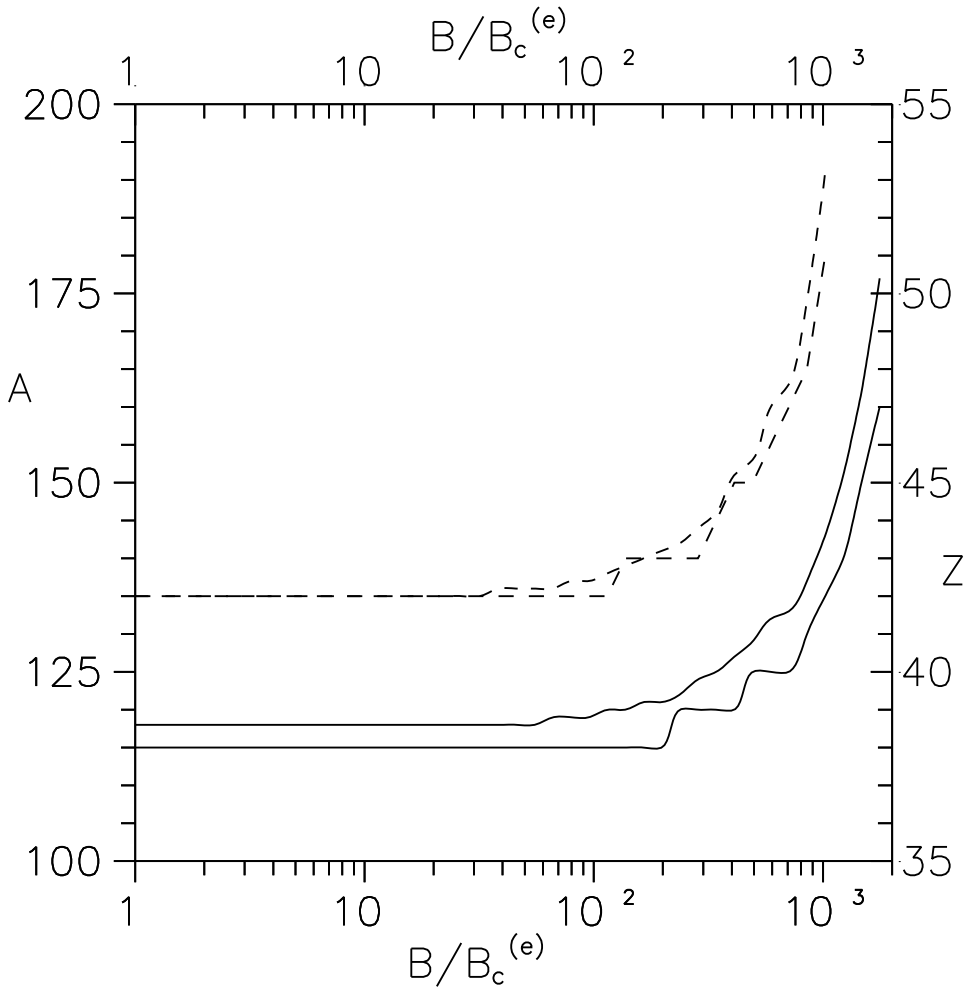

Variation of critical values for A and Z with the strength of magnetic field B (expressed as $B/B_c^{(e)}$) at which kinetic pressure becomes just zero. The solid curves are based on HW equation of state whereas the dashed curves are from BBP equation of state. In each case, the upper curve is for A and the lower one is for Z.

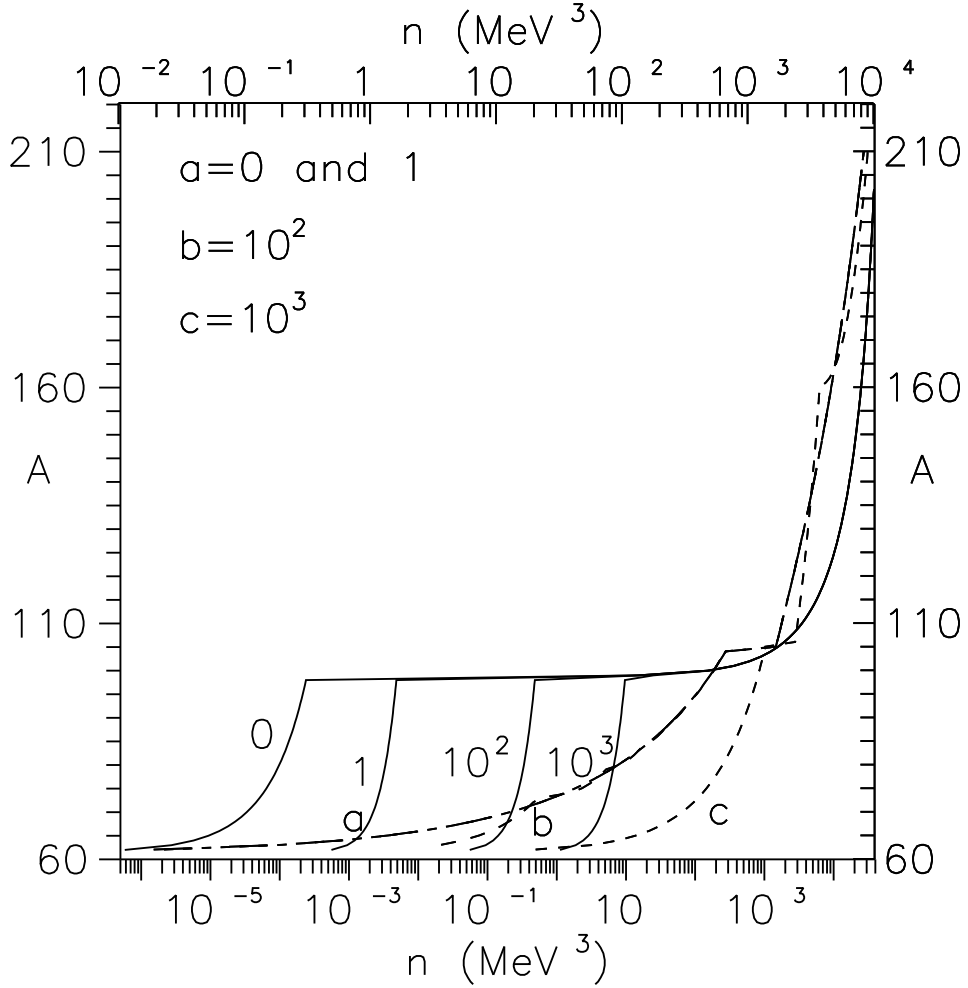

Variation of mass number of the nuclei with the total baryon density. HW equation of state: four different magnetic field strengths:$B = 0$, $B = 10B_c^{(e)}$, $B = 10^2 B_c^{(e)}$ and $B = 10^3 B_c^{(e)}$, indicated by 0, 1, 10^2 and 10^3 respectively. BBP equation of state: Dashed curves, the magnetic field strengths $B = 0$, $B = 10B_c^{(e)}$ (both are indicated by a), $B = 10^2 B_c^{(e)}$ (indicated by b) and $B = 10^3 B_c^{(e)}$ (indicated by c). Here, the lower x-axis is for HW equation of state and the upper one is for BBP equation of state.

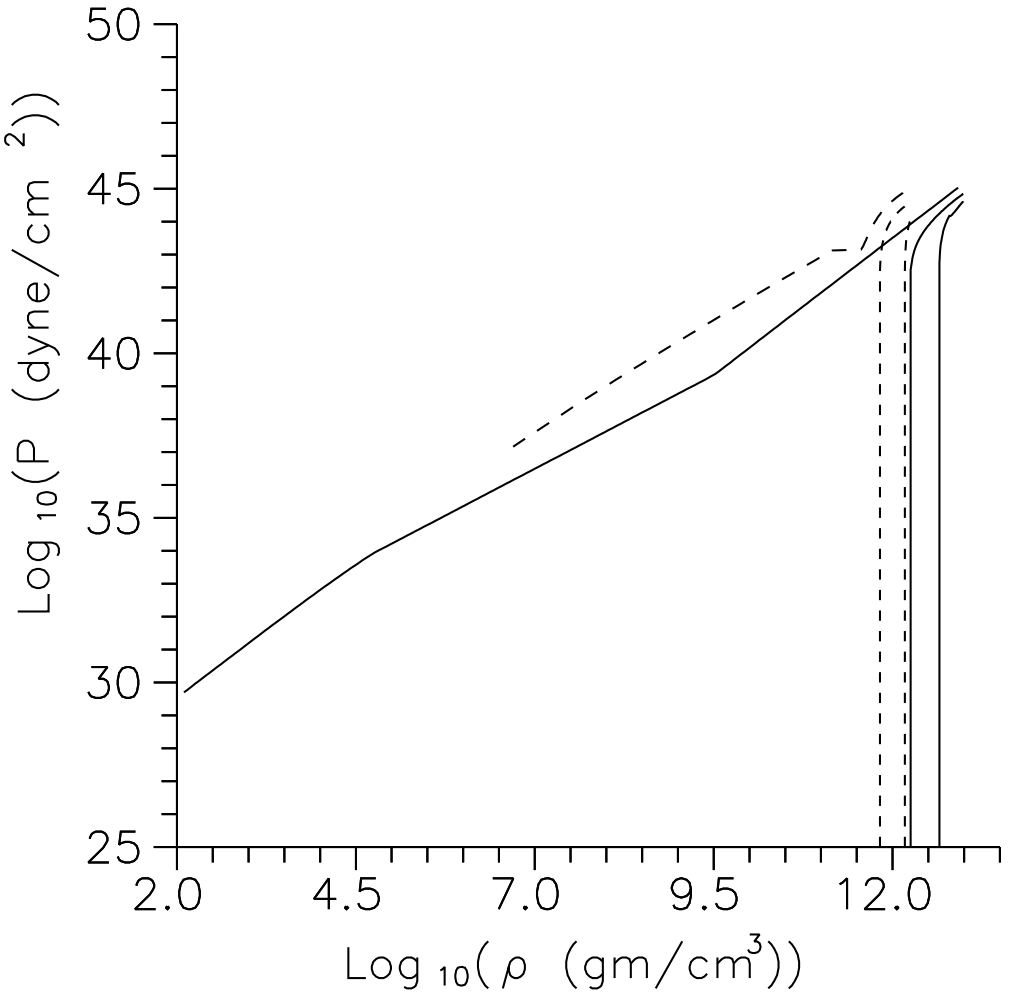

Equation of states from HW and BBP mass formulae. Solid curves are for HW equation of state, whereas, the dashed curves are for BBP case. For each case, the upper curve is for $B = 0$, middle and lower curves are for $B = B_c^{(e)}$ and $B = 10^3 B_c^{(e)}$ respectively.

Conclusions

- The upper limit of Landau quantum number is a function of positional coordinate of the electron within the WS cells.

- At the surface region, irrespective of magnetic field strength, this upper limit becomes identically zero $\Longrightarrow$ electrons near the WS cell surface are strongly polarized. For $B > 10^{15}$G, they are polarized at every points within the cells.

- For a stable strongly magnetized inner crust matter, the nuclei present must be heavier than iron and much more neutron rich. The heaviness is more in the case of BBP equation of state.

- For low and moderate values of magnetic field strength, the variation of mass number and the corresponding atomic number with magnetic field is not so significant. Whereas, for $B \geq 10^{14}$G, when electrons occupy only the zeroth Landau level, then much more heavier neutron rich nuclei are formed in the inner crust

region. It is found that high magnetic field behaves like a catalyst to generate heavy neutron rich nuclei.

- In the case of HW equation of state, free neutron density does not depend on the strength of magnetic field, whereas, for BBP case, because of chemical equilibrium condition, the free neutron density depends on the magnetic field strength. In the case of BBP equation of state the overall qualitative difference is because of chemical equilibrium among the constituents.

- The qualitative nature of equation of states are almost identical. It is found that in presence of strong magnetic field, the inner crust matter becomes mechanically stable at very high density.

- It is expected that the strong magnetic field, if present well within the inner crust of magnetars, must affect the super-fluidity of cold neutron matter.

Expulsion of Magnetic Flux Lines from a Type-I Superconducting Quark Star

(Nag & Chakrabarty, Astrphys. & Space Sc., 2007 & 2009)

- Quark matter $\longrightarrow$ constituents: colored quarks and gluons $\longrightarrow$ possible at extremely high temperatures and / or densities.

- If the $\rho_c = 3 - 4 \times \rho_0 \Longrightarrow$ phase transition to quark matter. Compact stars composed mostly or entirely of quark matter are called hybrid stars or quark stars.

- Micro-second after Big Bang the universe was supposed to be filled with hot phase of quark matter.

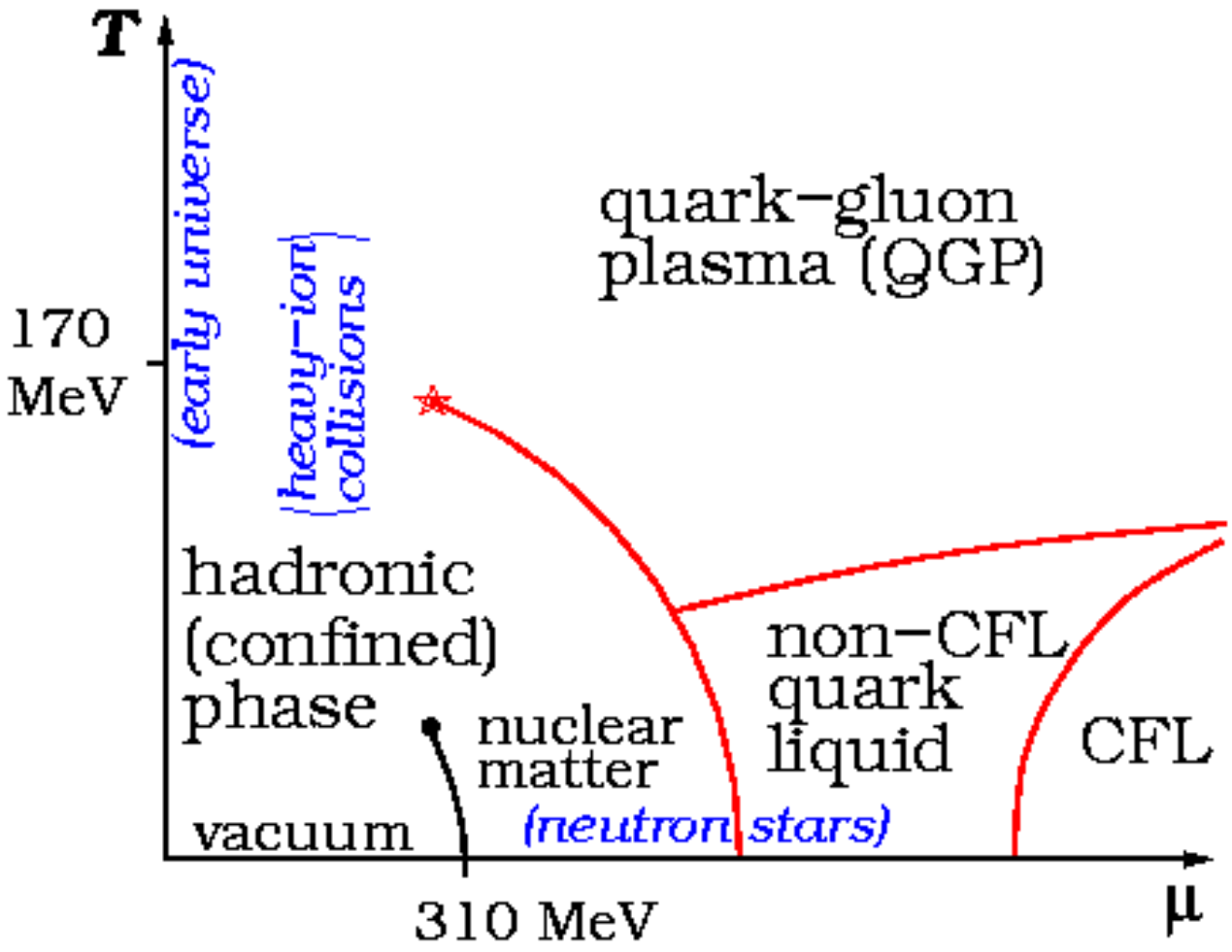

Schematic Diagram of QCD Phase Transition

(Witten, PRD, ’84, Ghosh & Chakrabarty, PRD, ’95,’96,’01, Chakrabarty et al, PRL, ’97,’98, Rajagopal & Wilczek, PRL, ’01)

(D. Bailin and A. Love, Phys. Rep. **107**, 325 (1984).)

- Many fermion microscopic theory of superconductivity: if the interaction favours formation of Cooper pairs at low temperature $\longrightarrow$ may undergo a phase transition to a super-conducting state.

- For quark matter: the basic interaction between quarks is attractive at large distances $\Longrightarrow$ BCS pairing mechanism is also applicable here in color space- color superconductivity.

- The transition is of type-I $\Longrightarrow$ By Meissner mechanism, the magnetic flux lines will be expelled from the superconducting zone.

- Critical magnetic field: $\sim 10^{16}$G, $\gg$ the typical pulsar magnetic field.

- Critical temperature: $\sim 10^{9} - 10^{10}$K, $\gg$ for quark stars.

- For a small type-I superconducting laboratory sample placed in an external magnetic field, less than the corresponding critical value, the expulsion of magnetic field takes place instantaneously.

- Whereas in the quark stars ($R = 10$Km) scenario, the picture may be completely different. It may take several thousands of years for the magnetic flux lines to get expelled from the superconducting core region. Which further means, that the growth of superconducting phase in quark stars will not be instantaneous.

- It is assumed that superconducting transition occurs from the centre, by the nucleation of a super-critical bubble of superconducting material in normal quark matter.

- The critical radius can be obtained from the difference of free energies

$$r_c = \frac{16\pi\alpha}{B_m^{(c)2}\left[1 - \left(\frac{B_m}{B_m^{(c)}}\right)^2\right]}$$

- $\alpha \longrightarrow$ surface tension ($10^{-3} \leq \alpha \leq 1$).

- $B_m^{(c)} \longrightarrow$ critical magnetic field.

- The dynamical equation for the flux expulsion at the sharp normal-superconducting interface:

$$\frac{\partial B_m}{\partial t} = D\nabla^2 B_m$$

- $D \sim 1/\sigma$, where $\sigma \sim 10^{26}$ sec$^{-1} \longrightarrow$ electrical conductivity of the normal phase.
  (P. Haensel, J.L. Zdunik and R. Schaeffer, Astr. and Astrophys. **160**, 121 (1986).)

- For steady expulsion, $\tau_D = 10^5 - 10^6$yrs $\longrightarrow \sim$ flux expulsion time scale.

- We compare this phenomenon of magnetic flux expulsion from a growing superconducting quark matter core with the diffusion of impurities from the frozen

phase of molten metal. The mechanism is used by the material scientists and metallurgists.

- Because of the accumulation of impurities at the dendritic tips near the interface, it becomes dynamically unstable. The dynamical theory of this solidification instability was first analyzed in 1964 in a seminal paper by Mullins and Sekerka and is called Mullins-Sekerka instability. (Mullins & Sekerka, J. Appl. Phys., '63, '64; Langer, Rev. Mod. Phys., '80)

- Due to the presence of excess magnetic flux lines at the interface, which is true because the diffusion rate of magnetic lines of forces in the normal phase may be less than the rate of growth of the superconducting zone, the topological structure of normal-superconducting boundary layer may change significantly. An identical type instability may be observed here also

- In the case of crystallization in the laboratory, one can observe the sharp interface, whereas, quark stars are several light years away from us, therefore such instability at the normal-superconducting interface has no physical significance

- The growth of super-critical superconducting nucleus: Stepwise attachments of Cooper pairs to the super-critical bubble: $A_n + A_1 \longrightarrow A_{n+1}$.

- $F(r,t) \longrightarrow$ characteristic size of the bubble $\longrightarrow$ Growth equation:

$$\frac{\partial F}{\partial t} = D_n \nabla^2 F$$

- $D_n \longrightarrow$ nuclear size diffusion coefficient.

- Steady growth or instability at the interface $\Longrightarrow$ controlled by the relative magnitudes of D and D_n.

- Steady expulsion from SC phase: Rate of expulsion from SC phase$\leq$ Rate of diffusion in normal phase, there will be no surface instability.

- For rate of diffusion is low, accumulation of excess magnetic lines of forces at the sharp interface $\Longrightarrow$ system may become energetically unstable if $B_m >$

critical value, $\Longrightarrow$ destruction of superconductivity. It is the special feature of this physical change.

- **A Comparison of Various Phases in Two Different Scenarios:**

  - The normal quark matter phase is compared with the molten alloy phase.

  - the formation of superconducting zone is compared with the freezing of molten alloy to pure metal.

  - Magnetic field lines in normal phase are compared with the impurities in molten alloys.

  - Free energy minimization: Impurity transport from solid pure metal phase to molten alloy. Analogously, magnetic lines of forces prefer to remain in normal quark matter phase $\Longrightarrow$ Meissner effect.

• **New Definition of Meissner Effect for a Bulk System:** Solubility of magnetic flux lines in the type-I superconducting phase is zero.

• To investigate the stability of the interface, we have obtained the magnetic field strength on the spherical interface for each radial coordinate. Assumption: Rate of growth $>$ rate of diffusion in normal phase

• We have taken a small area perpendicular to the interface at an arbitrary position for a given radial coordinate and obtained numerically the magnetic field strengths at every point on that area and are plotted in 3-d certisian coordinate system.

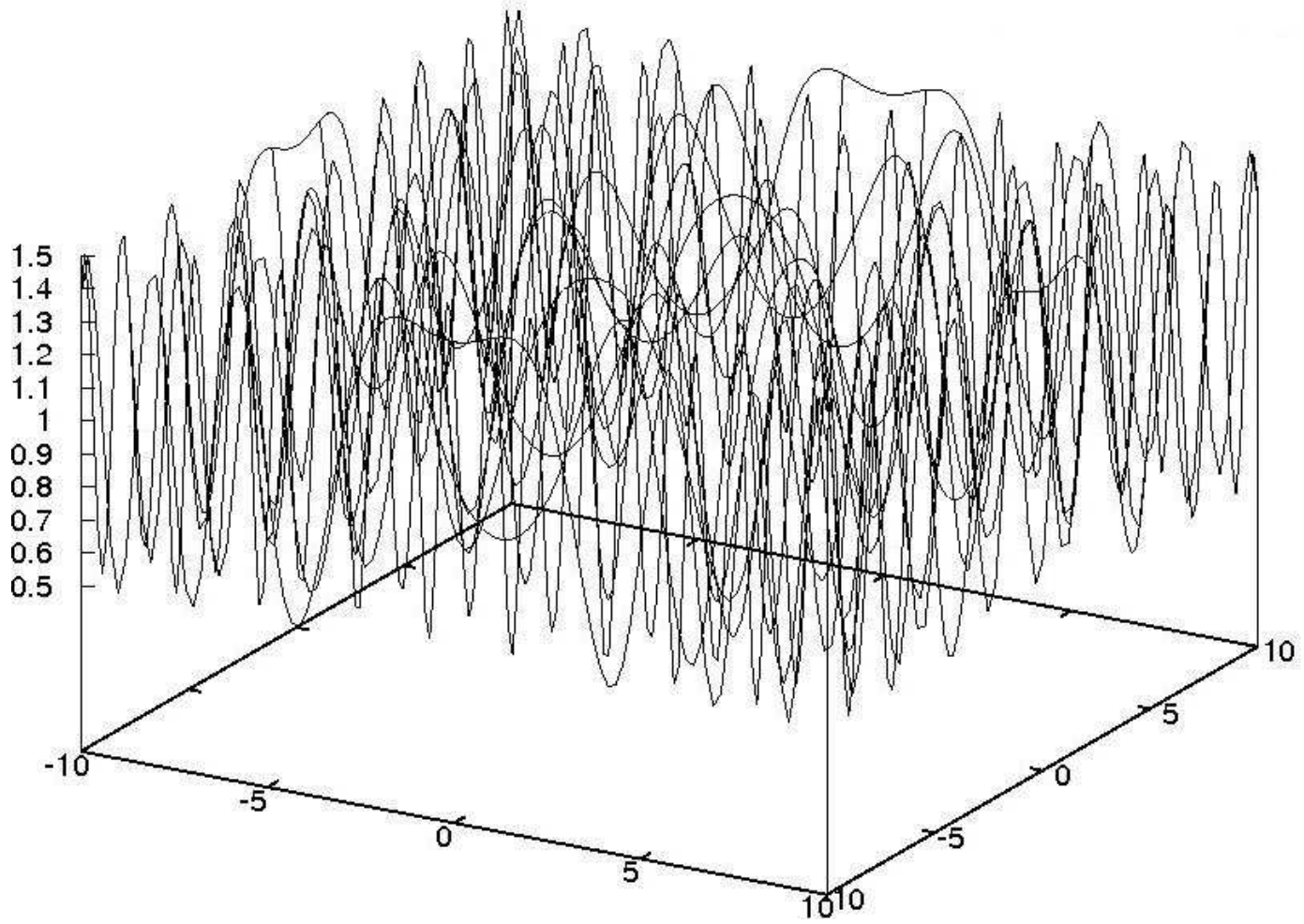

Distribution of Magnetic field at the superconducting-normal quark matter interface

Conclusion

- The magnetic properties of bulk astrophysical superconducting objects are entirely different from that of a small laboratory superconducting sample.

- Expulsion of magnetic flux lines from the superconducting zone is not instantaneous. The typical time scale is $10^5 - 10^6$ yrs. We have noticed that this time scale is very close to the magnetic field decay time scale in a neutron star.

- Due to the presence of excess magnetic flux lines at the interface, which is true if the diffusion rate of magnetic lines of forces in the normal phase is less than the rate of growth of the superconducting zone, the topological structure of normal-superconducting boundary layer may change significantly.

- The stability of planer interface also depends on the strength of magnetic field at the boundary layer.

- Since the expulsion time scale is very high, we expect that there will be no instability at the interface between normal and superconducting quark matter phase, provided the magnetic field at the core region just before superconducting phase transition is $\sim 10^{-3} \times B_m^{(c)}$. In this situation, the superconducting phase will grow steadily.